Acta Neuropathol (2011) 121:39–57
DOI 10.1007/s00401-010-0713-y

ORIGINAL PAPER

Genetic Creutzfeldt-Jakob disease associated with the E200K mutation: characterization of a complex proteinopathy

Gabor G. Kovacs · Jérémie Seguin · Isabelle Quadrio · Romana Höftberger · István Kapás · Nathalie Streichenberger · Anne Gaëlle Biacabe · David Meyronet · Raf Sciot · Rik Vandenberghe · Katalin Majtenyi · Lajos László · Thomas Ströbel · Herbert Budka · Armand Perret-Liaudet

Received: 1 April 2010 / Revised: 10 June 2010 / Accepted: 20 June 2010 / Published online: 1 July 2010

Abstract The E200K mutation is the most frequent prion protein gene (*PRNP*) mutation detected worldwide that is associated with Creutzfeldt-Jakob disease (CJD) and thought to have overlapping features with sporadic CJD, yet detailed neuropathological studies have not been reported. In addition to the prion protein, deposition of tau, α-synuclein, and amyloid-β has been reported in human prion disease. To describe the salient and concomitant neuropathological alterations, we performed a systematic clinical, neuropathological, and biochemical study of 39 individuals carrying the E200K *PRNP* mutation originating from different European countries. The most frequent clinical symptoms were dementia and ataxia followed by myoclonus and various combinations of further symptoms, including vertical gaze palsy and polyneuropathy. Neuropathological examination revealed relatively uniform anatomical pattern of tissue lesioning, predominating in the basal ganglia and thalamus, and also substantia nigra, while the deposition of disease-associated PrP was more influenced by the codon 129 constellation, including different or mixed types of PrP^{res} detected by immunoblotting. Unique and prominent intraneuronal PrP deposition involving brainstem nuclei was also noted. Systematic examination of protein depositions revealed parenchymal amyloid-β in 53.8%, amyloid angiopathy (Aβ) in 23.1%, phospho-tau immunoreactive neuritic profiles in 92.3%, neurofibrillary degeneration in 38.4%, new types of tau pathology in 33.3%, and Lewy-type α-synuclein pathology in 15.4%. TDP-43 and FUS immunoreactive protein deposits were not observed. This is the first demonstration of intensified and combined neurodegeneration in a genetic prion disease due to a single point mutation, which might become an important model to decipher the molecular interplay between neurodegeneration-associated proteins.

Keywords Alpha-synuclein · Amyloid-beta · Prion protein · Tau · Neurodegeneration

Electronic supplementary material The online version of this article (doi:10.1007/s00401-010-0713-y) contains supplementary material, which is available to authorized users.

G. G. Kovacs (✉) · R. Höftberger · T. Ströbel · H. Budka
Institute of Neurology, Medical University of Vienna, and Austrian Reference Center for Human Prion Diseases, AKH 4J, Währinger Gürtel 18-20, 1097 Vienna, Austria
e-mail: gabor.kovacs@meduniwien.ac.at

G. G. Kovacs · I. Kapás · K. Majtenyi
Neuropathology and Prion Disease Reference Center, Hungarian Reference Center for Human Prion Diseases, Semmelweis University, Budapest, Hungary

J. Seguin · I. Quadrio · N. Streichenberger · D. Meyronet · A. Perret-Liaudet
Prion Disease Laboratory, Pathology and Biochemistry, Groupement Hospitalier Est, Hospices Civils de Lyon/Claude Bernard University, Lyon, France

A. G. Biacabe
Agence Française de Sécurité Sanitaire des AlimentŝLyon, Unité ATNC, Lyon Cedex 07, France

R. Sciot
Department of Pathology, University Hospital, Catholic University of Leuven, Leuven, Belgium

R. Vandenberghe
Neurology Department, University Hospital Gasthuisberg, Leuven, Belgium

L. László
Department of Anatomy, Cell and Developmental Biology, Eotvos Lorand University of Sciences, Budapest, Hungary

Introduction

Prion diseases are acquired, sporadic or genetic in origin. Mutations in the prion protein (PrP) gene (*PRNP*) are associated with spongiform encephalopathy (Creutzfeldt-Jakob disease, CJD) or PrP amyloidosis (Gerstmann-Sträussler-Scheinker disease, or cerebral amyloid angiopathy) [37]. In addition to the mutation, the constellation at codon 129 (methionine/methionine, MM, or valine/valine, VV, homozygosity, MV heterozygosity) seems to influence phenotypes also in genetic prion diseases [42, 46]. The E200K mutation is the most frequent *PRNP* mutation detected worldwide that is associated with CJD [5, 21, 22, 41, 42, 49], with increased incidence among Libyan Jews and in Slovakia and Hungary [29, 33, 35, 40, 47, 49]. Examination of microsatellite markers indicated at least four different ancestral origins, with cases in Hungary or Slovakia differing in origin from those in Austria, France, or Belgium and other parts of the world [44]. Clinical presentations overlap with those described in sporadic CJD, furthermore, insomnia, vertical gaze palsy, and polyneuropathy were described as well [1, 2, 8, 42, 47, 50, 64].

Prion diseases are representatives of neurodegenerative diseases, which are classified by protein depositions such as α-synucleinopathies, tauopathies, TDP-43, or FUS proteinopathies, or diseases associated with the deposition of amyloid-β (Aβ). These proteinopathies show considerable overlap [36] and were described as concomitant pathologies in prion diseases as well. α-Synucleinopathies like Parkinson's disease (PD) are characterized by deposition in the brain of α-synuclein protein in the form of Lewy bodies and neurites that may be also detected in about 10% of subjects above 60 years, most likely representing presymptomatic PD [12]. An increased prevalence of Lewy bodies was found in elderly sporadic CJD (23.5%) and also in the acquired variant CJD [66]. Phospho-tau immunoreactive neuritic profiles around amyloid plaques are features of variant CJD [19]. Neurofibrillary tangle pathology, morphologically similar to Alzheimer's disease (AD), is associated with PrP gene (*PRNP*) mutations with prominent PrP amyloid deposition [17]. Moreover, abundant Aβ deposits may be detected in sporadic CJD with higher age and a specific clinicopathological profile [11]. Codistribution of Aβ and disease-associated PrP was recently demonstrated in three cases of E200K mutation of Hungarian origin [18].

There are studies summarizing clinical features [47, 63], furthermore, case reports on neuropathological alterations [8, 9, 26, 30, 45, 64] or evaluation of certain regions (e.g. cerebellum) [32, 49], and biochemical evaluations of protease-resistant PrP (PrP^{res}) [7, 27, 57] of individuals with CJD associated with E200K mutation. However, there is a paucity of systematic neuropathological evaluation of cases. Thus, in the present paper we report the results of a comprehensive and systematic clinical, neuropathological, and biochemical study of 39 individuals carrying the E200K *PRNP* mutation originating from different European countries. In addition to various types of PrP immunoreactivity, we found surprisingly high proportion of cases with various depositions of neurodegeneration-associated proteins (Aβ, phospho-tau, α-synuclein).

Materials and methods

Selection of cases

Within the European surveillance for human prion diseases, we systematically examined 39 patients (4 Austrian, 3 Belgian, 6 French, and 26 Hungarian) with confirmed E200K mutation in *PRNP*. Clinical and neuroradiological data were obtained retrospectively. These patients were notified as suspected CJD patients to the national surveillance network, using the current clinical criteria for CJD, and verified at postmortem. When a sign was indicated as absent, it means that it was checked and found negative. Genetic analysis was performed using genomic DNA isolated from blood samples or frozen brain tissue as published before, after informed consent to the patient or one of his relatives in the frame of CJD Surveillance [16, 35, 56].

Neuropathology

Formalin fixed, paraffin-embedded tissue blocks (2.5 × 2.0 cm) were evaluated. Post mortem delay was generally within 24 h except for three cases (48 h). The latter were not included in our biochemical studies. In addition to hematoxylin and eosin staining, the following monoclonal antibodies were used for immunohistochemistry: anti-tau AT8 (pS202, 1:200) AT100 (pS212, 1:200), AT180 (pT231, 1:200), HT7 (tau 169-163, 1:100; all from Pierce Biotechnology, Rockford, IL, USA), anti-phospho-TDP-43 (pS409/410, 1:2,000, Cosmo Bio, Tokyo, Japan), anti-α-synuclein (1:10,000, clone 4D6, Signet, Dedham, MA, USA), anti-Aβ (1:50, clone 6F/3D, Dako, Glostrup, Denmark), anti-PrP (1:1,000, 12F10, Cayman Chemical, Ann Arbor, MI, USA), anti-4R tau (RD4, 1:200, Upstate, Charlottesville, VA, USA), and anti-3R tau (RD3, 1:2,000, Upstate). In addition, we used the following polyclonal antibodies: anti-Aβ-40 (1:200) and anti-Aβ-42 (1:50; both Signet, Dedham, MA, USA), and anti-FUS (1:1000, Sigma, St. Louis, MO, USA). The DAKO EnVision© detection kit, peroxidase/DAB, rabbit/mouse (Dako, Glostrup, Denmark) was used for visualization of antibody reactions. Examined anatomical regions are summarized in Table 1. Neuropathological alterations (spongiform

Table 1 Summary of anatomical regions examined using different antibodies for immunostaining

Anatomical region/antibody	PrP	pTau	α-Syn	Aβ	pTDP-43	FUS	Ubi
Frontal cortex	+	+	+	+	+	+	+
Cingular cortex	+	+	+	−	−	−	−
Parietal cortex	+	−	−	−	−	−	−
Temporal cortex	+	+	+	+	−	−	−
Occipital cortex	+	+	−	+	−	−	−
Hippocampus CA subregions	+	+	+	+	+	+	+
Dentate gyrus	+	+	+	+	+	+	+
Subiculum	+	+	+	+	+	+	+
Entorhinal cortex	+	+	+	+	+	+	+
Caudate nucleus	+	+	+	+	−	−	−
Putamen	+	+	+	+	−	−	−
Globus pallidus	+	+	+	+	−	−	−
Thalamus medial nuclei	+	+	−	−	−	−	−
Thalamus lateral nuclei	+	+	−	−	−	−	−
Substantia nigra	+	+	+	−	+	+	+
Dorsal raphe nucleus	+	+	+	−	−	−	−
Locus coeruleus	+	+	+	−	−	−	−
Pontine base nuclei	+	+	+	−	−	−	−
Inferior olives	+	+	+	−	−	−	−
Hypoglossus nucleus	+	+	+	−	−	−	−
Dorsal vagus nucleus	+	+	+	−	−	−	−
Dentate nucleus	+	+	+	+	+	+	+
Cerebellar cortex	+	+	+	+	+	+	+

change, astrogliosis, neuronal loss, and degree of various protein depositions) were semiquantitatively (none, mild, moderate, severe) evaluated in all examined anatomical regions.

Double immunolabeling was performed using monoclonal PrP (12F10, 1:300), Abeta (1:20, Dako), Tau AT8 (1:100), SMI-31 (1:2000, Covance, Berkeley, CA), Map-2 (1:250, Millipore Corp., Billerica, MA), HLA-DR (1:50, Dako), and polyclonal GFAP (1:1500, Dako). The fluorescence-labeled secondary antibodies were Alexa Fluor (AF) 555 donkey anti-mouse IgG (1:200; Molecular Probes, Inc., Eugene, OR, USA), AF 488 goat anti-rabbit (1:200; Molecular Probes, Inc.), and Zenon AF 488 Mouse IgG_1 (Molecular Probes, Inc.). The following combinations were applied: PrP (AF 555)/Tau (Zenon 488); PrP (AF 555)/Abeta (Zenon 488); HLA-DR, SMI-31, and Map-2 (AF 555)/Tau (Zenon 488), and Tau (AF 555)/GFAP (AF 488). Double immunolabeling involving anti-PrP antibody was performed after pretreatment of the section with 20 min heat-induced epitope retrieval with citrate buffer (pH 6) followed by 2 min formic acid (96%); for all others 20 min heat-induced epitope retrieval with citrate buffer was used. We evaluated double immunofluorescent labeling with a Zeiss LSM 510 confocal laser microscope.

Immunoblotting

Prion protein

Western blot analysis was performed as previously described with minor modification [58]. Briefly, 20% cortical gray matter homogenates were obtained using buffer containing 5% glucose in ultra pure grade water. Homogenates were diluted twofold in buffer [100 mM Tris (pH 7.4), 0.5% glucose, 0.9% NaCl] and digested with proteinase K (25 μg/ml) for 1 h at 37°C before stopping digestion by 1 mM PMSF. Digested homogenates were further ultracentrifuged (Sorvall Discovery M150 SE, Thermo, USA) in *N*-lauryl-sarcosyl (final concentration of 10%) for 75 min at 140,000 rpm. Pellets were resuspended with a denaturing buffer (125 mM Tris, 4% SDS, 20% glycerol), heated for 5 min at 100°C and centrifuged at 12,000*g* for 10 min. The supernatant was collected for western blot analysis. Samples and biotinylated molecular mass marker (SIGMA, range 14.3–97.0 kDa) were run on 16% SDS-PAGE gels. In addition, selected samples were also run on a 12% gel. All immunoblots were incubated with the monoclonal antibody 3F4 (recognizing the epitope at PrP residues 108–111) at a concentration of 0.1 μg/ml (Proteinogenics, USA), followed by incubation with a goat anti-mouse IgG horseradish peroxidase (HRP) conjugated antibody and detection using a chemiluminescent substrate (Supersignal Dura, Pierce, USA).

Tau

Frozen brain tissue from four neuropathologically confirmed E200K genetic CJD patients (3 French and 1 Hungarian), one confirmed AD patient and one control brain from an individual lacking tau pathology was obtained. Insoluble tau fraction was extracted as described [28] with some modifications. Briefly, 20% cortical gray matter homogenates were prepared using a buffer containing 50 mM Tris (pH 7.4), 0.8 M NaCl, and 10 mM EGTA. Homogenates were centrifuged at 100,000*g* for 25 min and the resulting pellets were homogenized in 1 mL of buffer containing 10 mM Tris (pH 7.4), 0.85 M NaCl, 1 mM EDTA, 20 mM NaF and 10% sucrose. Following centrifugation for 25 min at 20,000 rpm, sarkosyl was added to supernatants to a final concentration of 1%. After incubation at RT for 2 h, the supernatants were centrifuged at 100,000 rpm for 45 min. The sarkosyl-insoluble pellets were suspended in 50 μL Laemmli buffer and heated for 10 min at 100°C.

Table 2 Summary of clinical and demographic data

Features	*PRNP* codon 129			All**
	MM	MV	VV	
Number of cases	21 (58.3%)	14 (38.9%)	1 (2.8%)	36/39
Women	14 (35.8%)	5 (12.8%)	1 (2.5%)	22 (56.4%)
Men	7 (17.9%)	9 (23%)	0	17 (43.6%)
Age at death (mean ± SE)	59.76 ± 2.27	60.64 ± 1.81	66.0	60.28 ± 1.49
Duration of illness (mean ± SE)	4.20 ± 0.60	5.77 ± 0.84	4.0	4.79 ± 0.48
Age range	33–76	46–74	66.0	33–76
Duration of illness range	2–12	1–13	4	1–13
Dementia	17 (81%)	14 (100%)	1	35 (89.7%)
Ataxia	16 (76.2%)	12 (85.7%)	1	32 (82.1%)
Myoclonus	13 (61.9%)	5 (35.7%)	1	20 (51.3%)
Pyramidal signs	10 (47.6%)	5 (35.7%)	0	15 (38.5%)
Rigidity/Parkinsonism	2 (9.5%)	3 (21.4%)	0	6 (15.4%)
Chorea/Dystonia	9 (42.9%)	4 (28.6%)	0	14 (35.9%)
Gaze palsy	3 (14.3%)	1 (7.1%)	0	4 (10.3%)
Insomnia*	2 (9.5%)	1 (7.1%)	0	3 (7.7%)
Early psychiatric symptoms	5 (23.8%)	2 (14.3%)	0	7 (17.9%)
Early behavioral change	5 (23.8%)	1 (7.1%)	1	7 (17.9%)
Polyneuropathy	2 (9.5%)	3 (21.4%)	0	6 (15.4%)
EEG: PSWC	10/19 (52.6%)	4/13 (30.8%)	0	15/35 (42.9%)
MRI: high signal in striatum	6/12 (50%)	2/6 33.3%)	1	9/19 (47.3%)
MRI: high signal in thalamus	2/12 (16.7%)	2/6 (33.3%)	0	4/19 (21%)

Duration of illness is given in months, age at death in years

From the 39 cases involved in the study, clinical information in one case and in three data on codon 129 were not available

PSWC periodic sharp wave complexes with triphasic morphology

* Reported prominent insomnia without polysomnography

** Including cases where there was a lack of data on codon 129

Samples were run on 4–12% gradient SDS-polyacrylamide gels (NuPAGE, Invitrogen). Proteins then were transferred onto Immobilon-P membranes (0.45 μm pore size, Millipore) and blocked overnight at 4°C. Afterwards, the membranes were incubated using the following primary antibodies: Anti-tau T46 (Signet, Dedham, MA, USA; 1:2,000 in PBS containing 0.5% Tween-20 and 0.5% dry milk) is a monoclonal antibody [34] raised against all six isoforms of human tau recognizing both recombinant human tau and PHF-tau on immunoblots; the phospho-dependent anti-Tau AT8 (Innogenetics, Gent, Belgium; 1:1,000 in PBS containing 0.1% Tween-20 and 0.5% dry milk) is a monoclonal antibody [20] directed against both Ser202 and Thr205 phospho-epitopes of tau; for the analysis of repeat isoforms in insoluble tau we used clone 8E6/C11 for the detection of three-repeat isoform RD3 of tau [10] (Millipore, Temecula, CA, USA; 1:1,000 in TBS containing 0.05% Tween-20 and 0.5% dry milk) and clone 1E1/A6 for the detection of four-repeat isoform RD4 of tau [65] (Millipore, Temecula, CA, USA; 1:1,000 in TBS containing 0.05% Tween-20 and 0.5% BSA). After incubation with a goat anti-mouse IgG horseradish peroxidase (HRP) conjugated antibody (Jackson Immunoresearch Laboratories, Inc., West Grove, PA, USA) at a final dilution of 1/10,000, immunological detection was performed using chemiluminescence technology according to the manufacturer's instructions (Pierce Biotechnology, Rockford, IL, USA).

Statistical analysis

Duration of illness, age at death, scores of neuropathological variables in different groups were compared using one-way ANOVA test or χ^2 test.

Results

Summary of clinical and genetic data

Clinical data were available for 38 (out of 39) patients (Table 2). Analysis of *PRNP* codon 129 was available for 36 patients. Age at death did not differ between constellations of codon 129, while the duration of illness was longer in patients with MV at codon 129, although in our cohort it did not reach the level of significance ($p > 0.05$). The most frequent clinical symptoms were dementia and ataxia followed by myoclonus and various combinations of further symptoms. Prominent vertical gaze palsy was described in 10.3% of patients, and polyneuropathy (axonal and rarely demyelinative) was noted in 15.4%, while early psychiatric symptoms or behavioral change was also noted in approximately one-fifth of individuals. Cranial MRI images were available for one-third of the patients; high signal in the basal ganglia was noted in approximately half of the patients, while high signal in the thalamus was seen

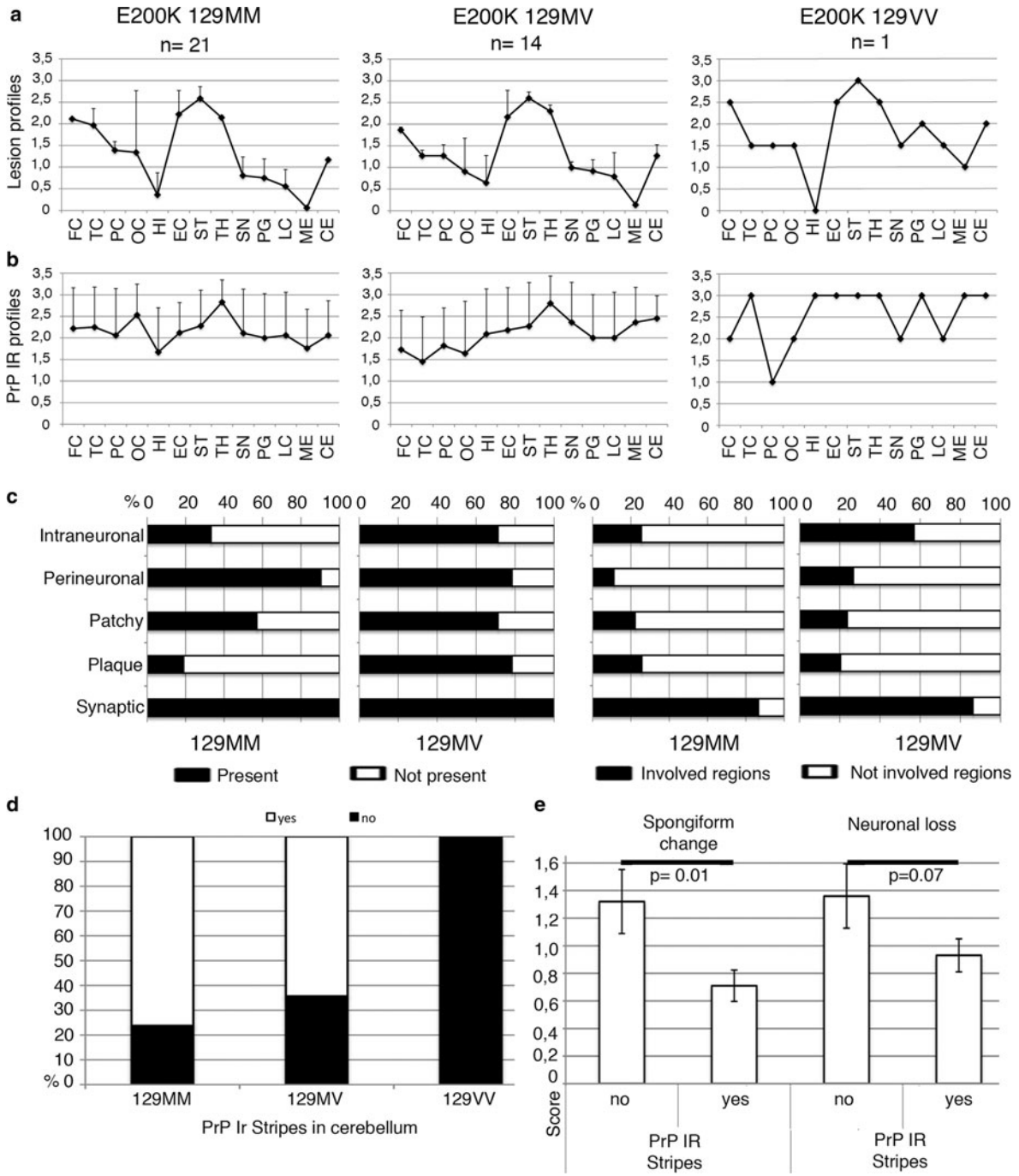

Fig. 1 Lesion and PrP immunoreactivity profiles and anatomical correlations of PrP immunoreactivities in E200K genetic CJD cases grouped according to the codon 129 polymorphism. **a** Lesion profiles [53] obtained by averaging the three scores (see text) for spongiform change, neuronal loss, and gliosis in the following gray matter regions: frontal cortex (*FC*), temporal cortex (*TC*), parietal cortex (*PC*), occipital cortex (*OC*), hippocampus CA1 subregion (*HI*), entorhinal cortex (*EC*), neostriatum (*ST*), medial thalamus (*TH*), substantia nigra (*SN*), midbrain periaqueductal gray (*PG*), locus coeruleus (*LC*), medulla oblongata (*ME*), cerebellum (*CE*). **b** PrP immunoreactivity profiles obtained by averaging the scores of different PrP immunoreactivities in the same regions indicated in **a**. **c** Percentage of cases with E200K genetic CJD grouped according to the polymorphism at codon 129 with or without different kinds of PrP immunoreactivities (two graphs on the *left side*) and the percentage of involved regions showing different PrP immunopositive patterns (two graphs on the *right side*). **d** Distribution of cases showing stripe-like PrP deposition in the molecular layer of the cerebellum in different groups (according to codon 129 polymorphism) of E200K genetic CJD cases. **e** Comparison of scores of spongiform change and neuronal loss in the cerebellar molecular layer and granular layer, respectively, in E200K genetic CJD cases with or without stripe-like pattern of PrP immunoreactivity

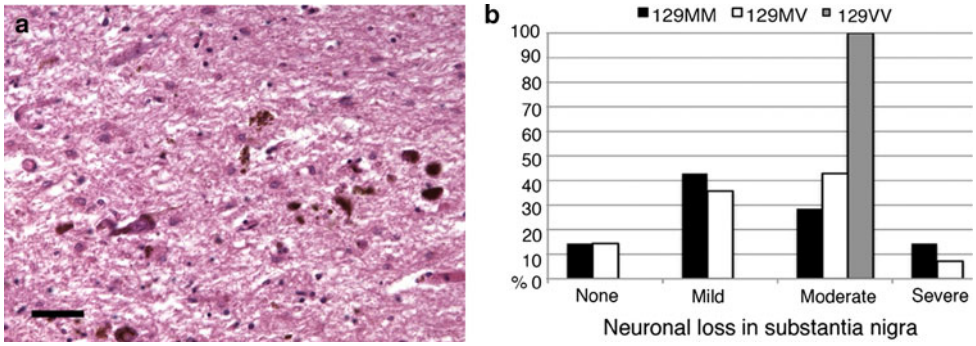

Fig. 2 Neuropathological alterations in the substantia nigra. **a** Neuronal loss and extracellular pigment in the substantia nigra in a representative case (*bar graph* indicates 30 μm). **b** Distribution of cases with none, mild, moderate or severe lesioning in the substantia nigra

in four patients, two of them with thalamic signal that was higher than in the basal ganglia, and was reminiscent of the pulvinar sign described in variant CJD [39]. Periodic sharp wave complexes with triphasic morphology were described in 43% of the patients' EEGs.

Neuropathological alterations

Spongiform change, neuronal loss and reactive astrogliosis of variable degree were observed in all cases. Vascular pathology with infarctions was seen in two cases. The distribution of spongiform change was relatively uniform in all patients irrespective of the constellation at codon 129 (Fig. 1a). In addition to neocortical regions, caudate nucleus, putamen and thalamic nuclei were most severely affected. In the cortex the deeper layers were frequently more involved, while in the hippocampal region, subiculum and entorhinal cortex had most tissue lesioning. Interestingly, the cerebellar cortex was relatively preserved in many cases. Gliosis and neuronal loss followed the degree of spongiform change, but predominated over spongiform change in the thalamus, particularly in brainstem nuclei (see supplemental Fig. 1a). Neuronal loss with extracellular pigment was frequently seen not only in the substantia nigra (Fig. 2a) but also in the locus coeruleus and dorsal raphe nucleus. Indeed, many cases with MM or MV at codon 129 showed moderate (28% MM, 42% MV) or severe (14% MM, 7% MV) lesioning in the substantia nigra, and only 15% of the cases in each group exhibited preserved neurons (0 score) (Fig. 2b). One case showed severe damage of the cortex with myelin loss and gliosis in the white matter compatible with a panencephalopathic form of CJD (62-year-old Belgian patient with 14 months duration of disease).

Characterization of proteinopathies

Prion protein

Immunohistochemistry Immunostaining for PrP revealed diffuse/synaptic deposits, patchy aggregates in the neuropil or around vacuoles, plaques without amyloid characteristics, fine perineuronal immunodeposits, and prominent intraneuronal dots (Fig. 3a–e). In cortical areas, laminar accentuation of PrP immunoreactivity was evident in many cases (Fig. 3f); synaptic or absence of PrP immunoreactivity frequently alternated with small foci showing prominent patchy aggregates of PrP (Fig. 3g). Of note was the frequent coarse deposition in medial thalamus (Fig. 3h). Prominent immunodeposition (synaptic and intraneuronal type) was noted in brainstem nuclei (Fig. 3i) and other subcortical areas (Fig. 3j). Although the involvement of regions was not significantly different between cases (Fig. 1b) and synaptic PrP immunoreactivity was seen in all cases, plaque-like structures and intraneuronal PrP immunodeposition predominated in cases with MV at codon 129 (Fig. 1c, supplemental Fig. 1b), particularly in the cortex. Plaque-like structures were more frequent in the hippocampus (Fig. 3k). When present, intraneuronal immunoreactivity always involved brainstem nuclei and showed prominent layer difference (deep layers > upper layers) in the cortex (see supplemental Fig. 1c). In the cerebellum, majority of the cases showed prominent PrP immunoreactivity restricted to the molecular layer in a stripe-like pattern [32] (Fig. 1d). Interestingly, these cases showed less prominent spongiform change in the molecular layer and less neuronal loss in the granular layer in comparison to cases with diffuse/synaptic PrP immunoreactivity involving all layers (Figs. 3l–o, 1e).

Western blot analysis of PrP^{res} Six French and four Hungarian subjects with confirmed prion diseases associated with E200K mutation on the *PRNP* gene were examined. Six individuals were methionine (MM) homozygous at codon 129 and 4 were heterozygous (methionine/valine, MV). E200K mutation was coupled with methionine at codon 129 in all cases. One further Austrian case homozygous for valine (VV) at codon 129 was published before [26].

The molecular type of PrP^{res} was determined by comparison with PrP^{res} type 1 and type 2 from the prefrontal cortex of two patients with sporadic CJD as reference

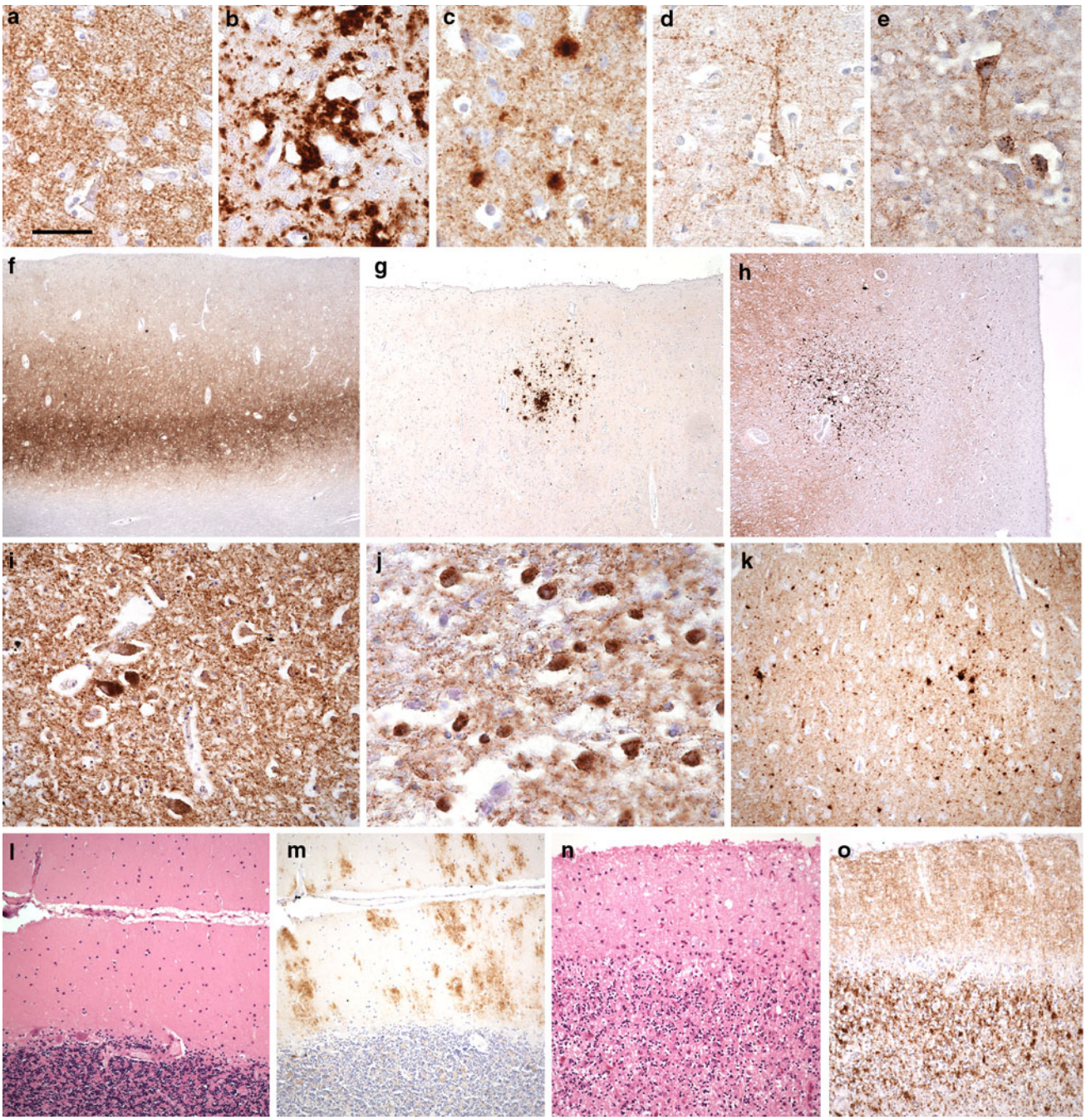

Fig. 3 Immunostaining for disease-associated prion protein. Immunostaining for PrP reveals diffuse/synaptic deposits (**a**), patchy/perivacuolar aggregates in the neuropil (**b**), plaque-like structures without amyloid characteristics (**c**), fine perineuronal immunodeposits (**d**), and prominent intraneuronal dots (**e**). In cortical areas laminar accentuation of PrP immunoreactivity is evident in many cases (**f**). In circumscribed cortical areas prominent patchy aggregates of PrP are seen (**g**). Coarse aggregates are frequent in the medial thalamus (**h**). Prominent immunodeposition (synaptic and intraneuronal type) in the locus coeruleus (**i**) and the lateral geniculate body (**j**). Plaque-like structures are frequent in the hippocampus (**k**). In the cerebellum less prominent spongiform change and neuronal loss (**l**, H&E) are associated with a stripe-like pattern of PrP immunoreactivity in the molecular layer of the cerebellum (**m**), contrasting those with obvious spongiform change and neuronal loss (**n**, H&E) and diffuse/synaptic PrP immunoreactivity (**o**). *Bar graph* in **a** indicates 60 μm for **a–e** and **i–k**, 500 μm for **g**, **h**, 1,000 μm for **f**, and 150 μm for **l–o**

standard (MM type 1 and VV type 2) [53]. The PrP^{res} patterns observed in these patients with the E200K mutation appeared distinct from the PrP^{res} pattern of patients with sporadic CJD PrP^{res} type 1 and type 2. These atypical patterns were apparently linked to an increase in the amounts of diglycosylated bands and a lower representation

of the unglycosylated one, associated with a discrete closeness between the di- and the monoglycosylated bands (Fig. 4).

The measurement of molecular masses in comparison to a molecular mass standard ladder loaded on SDS-PAGE in three wells clearly showed no difference between PrP^{res} type 1 in sporadic CJD and the PrP^{res} from E200K mutation. The difference of molecular masses calculated between the PrP^{res} type 1 and type 2 was 1.27 ± 0.06 kDa when samples were run in 16% gels. Interestingly, for three patients (2 MV and one MM at codon 129), we found a PrP^{res} with a type halfway between type 1 and type 2 of Parchi's classification [53], the difference between PrP^{res} type 1 and PrP^{res} from these patients (arbitrarily termed type 1* here) was 0.7 kDa (Fig. 4a). Running electrophoresis on 12% gels of these samples, this type 1* PrP^{res} was similar to type 1 of that described by Parchi et al. [53] in sporadic CJD (Fig. 4b).

Most genetic cases studied here presented a PrP^{res} type similar to type 1 (7/10 patients E200K) whereas one presented a type 2 (MV at codon 129) in the cerebellum, thalamus, frontal, and occipital cortex, and two cases showed mixed PrP types: one case (MV at codon 129) exhibited type 2 PrP^{res} in occipital, frontal, and temporal cortex, but type 1 in the cerebellum, thalamus, striatum, and cingulate gyrus (Fig. 4c); another case (MM at codon 129) showed mainly type 1 PrP^{res} but with co-ocurrence of types 1 and 2 in frontal cortex. These patterns correlated well with coarse and fine immunodeposits seen in immunohistochemistry.

Tau pathology

Immunoreactivity for phosphorylated tau: three patterns of tau pathology as seen by immunostaining for AT8 (summarized in Fig. 5)

1. In 36 cases (93.3%), neuritic profiles were immunostained, mainly in areas with more prominent tissue pathology, neuronal loss and spongiform change (Fig. 6a), including the posterior horn of the spinal cord in the single case where spinal cord was available.
2. In addition, in 15 cases (38.4%) neurofibrillary degeneration (Fig. 6b) following Braak and Braak stages were observed. Three further cases showed neurofibrillary tangles restricted to the dorsal raphe nucleus and locus coeruleus.
3. Furthermore, 13 cases (33.3%) showed features of a tauopathy that does not fulfill criteria of established sporadic tauopathy entities. This could be further subdivided as follows:

   (a) Six cases with neurofibrillary tangles, diffuse cytoplasmic tau immunoreactivity (pretangle-like), and threads in the caudate nucleus, putamen (Fig. 6c), brainstem (substantia nigra, dorsal raphe nucleus, and locus coeruleus) (Fig. 6d, e), and less in the thalamus, including one with

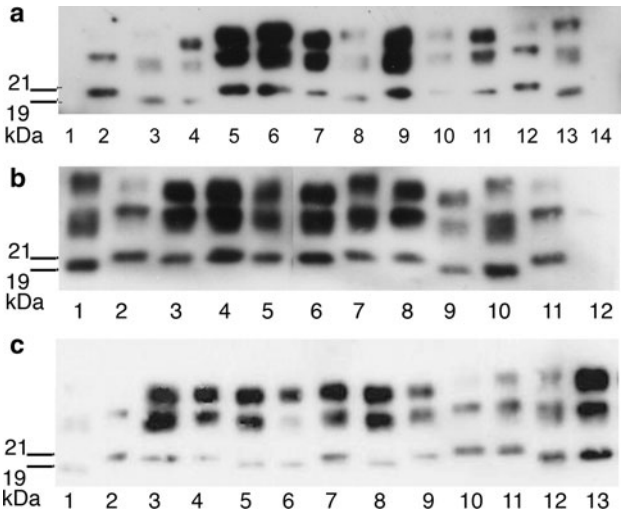

Fig. 4 Immunoblotting for disease-associated prion protein in representative cases. **a** PrP^{res} was extracted from different brain areas; after separation in 16% gels in denaturated conditions, PK resistant fragment of PrP were labeled by 3F4 anti prion antibody. *Lanes 1* and *14* negative control from non CJD patient, *Lanes 2* and *12* type 1 PrP^{res} control from sporadic CJD, *Lanes 3* and *13* type 2 PrP^{res} control from sporadic CJD, *Lane 4* 50 µg of thalamus from a French E200K CJD patient (MV at codon 129), *Lane 5* 0.7 mg of frontal from a Hungarian E200K CJD patient (MM at codon 129), *Lane 6* 1 mg of cerebellum from a Hungarian E200K CJD patient (MM at codon 129), *Lanes 7* and *11* type 1-like PrP^{res} (see text) from a French E200K patient (MV at codon 129), *Lane 8* type 2 PrPres control from sporadic CJD, *Lane 9* type 1-like PrP^{res} from 100 µg of cerebellum from a Hungarian E200K CJD patient (MV at codon 129), *Lane 10* type 1-like PrP^{res} (250 µg) from a Hungarian E200K CJD patient (MM at codon 129). **b** After initial running in 16% gels, some PrP^{res} types were confirmed after separation in 12% gels in denaturated conditions; PK resistant fragment of PrP were labeled by 3F4 anti prion antibody. *Lanes 1* and *10* type 2 PrP^{res} control from sporadic CJD, *Lanes 2* and *11* type 1 PrP^{res} control from sporadic CJD, *Lane 3* 50 µg of thalamus from a French E200K CJD patient (MV at codon 129), *Lane 4* 250 µg of frontal cortex from a Hungarian E200K CJD patient (MM at codon 129), *Lane 5* 100 µg of cerebellum from a Hungarian E200K CJD patient (MV at codon 129), *Lane 6* type 1 PrP^{res} control from a French E200K patient, *Lane 7* 1 mg of cerebellum from a Hungarian E200K CJD patient (MM at codon 129), *Lane 8* 0.7 mg of frontal cortex from a Hungarian E200K CJD patient (MM at codon 129), *Lane 9* 50 µg of thalamus from a French E200K CJD patient (MV at codon 129), *Lane 12* negative control from non CJD patient. **c** Western blot analysis of seven different brain areas from one E200K M129V CJD patient (*lanes 3–9*), probed with 3F4 anti-PrP mAb. Controls: *lanes 1* and *12* PrP^{res} type 2a (sporadic CJD), *lane 2* control PrP^{res} type 1 (sporadic CJD), *lane 10* control PrP^{res} type 1 (genetic CJD-E200K), *lane 13* control PrP^{res} type 2b (variant CJD), *lane 3* type 1 PrP^{res} from cerebellum (1 mg), *lane 4* type 1 PrP^{res} from striatum (100 µg), *lane 5* type 2a PrP^{res} from frontal (250 µg), *lane 6* type 2a PrP^{res} from occipital cortex (16 µg), *lane 7* type 1 PrP^{res} from thalamus (16 µg), *lane 8* type 2a PrP^{res} from temporal (250 µg), *lane 9* type 1 PrP^{res} from cingulate (50 µg)

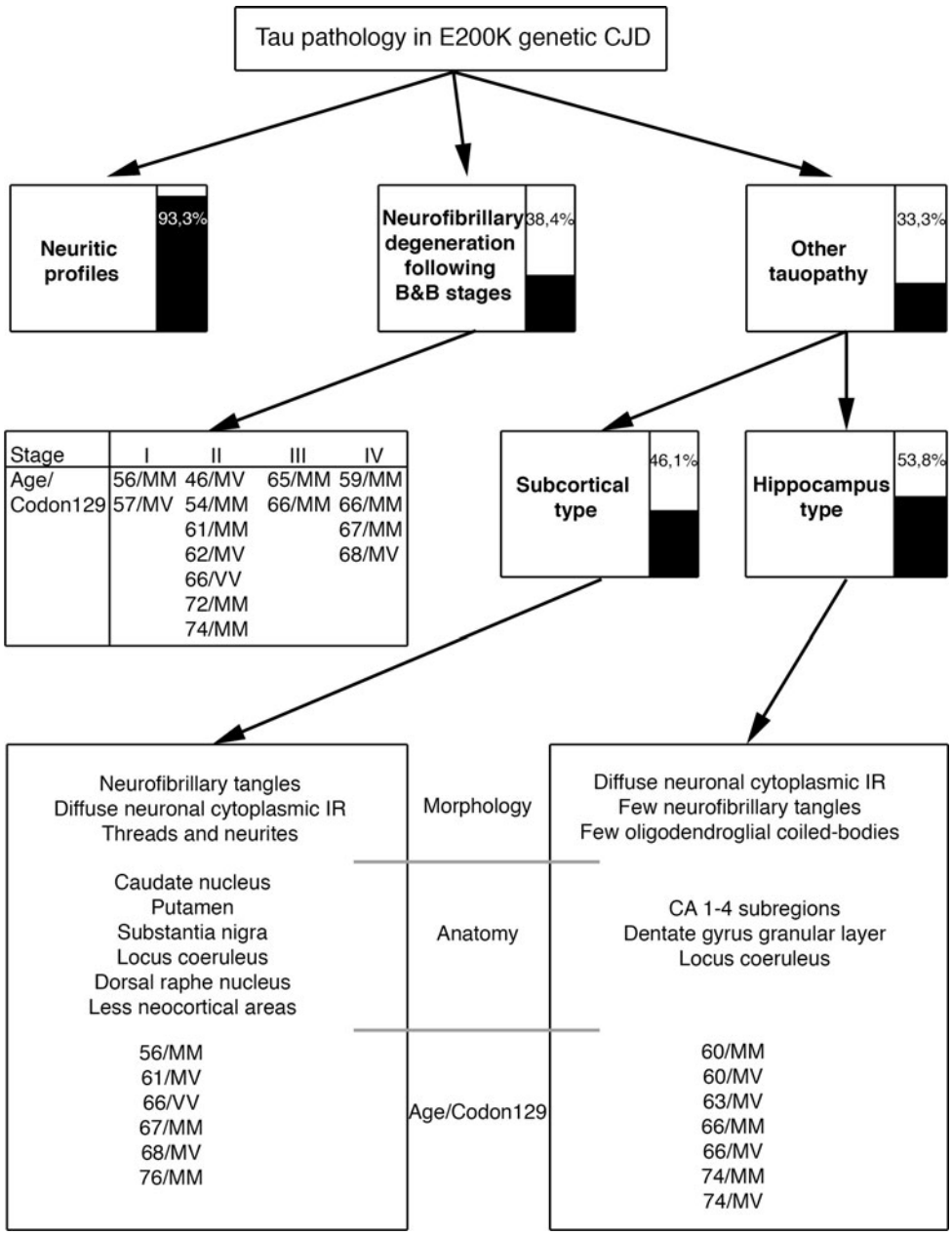

Fig. 5 Stratification of tau pathology in E200K genetic CJD according to cytopathology, regional distribution, age, and codon 129 polymorphism

prominent involvement of neocortical regions (Fig. 6f). There was lack of astrocytic plaques or tufted astrocytes, although some dot-like immunostaining of astrocytic processes were noted. Oligodendroglial coiled bodies were only occasionally seen.

(b) Seven further cases had an unusual distribution of neuronal and glial tau deposition in the hippocampus, which included neurofibrillary tangles and prominent diffuse neuronal granular cytoplasmic immunoreactivity not only in CA4, CA3, and CA2 subregions and dentate gyrus, but also in the CA1 subregion and subiculum, without or with scant neurofibrillary degeneration in the entorhinal cortex (Fig. 6g–i). In these cases argyrophilic grains were not seen, but some oligodendroglial tau immunopositivity and dot-like immunolabeling of astrocytic processes were observed. Interestingly, these cases also showed neurofibrillary tangles in the locus coeruleus.

Immunostaining for different anti-tau antibodies and co-localization studies Neuritic profiles were detected using immunostaining for 3R tau and less for 4R (Fig. 6j). Tau immunoreactive neurites occasionally co-localized with disease-associated PrP (Fig. 7a). Globose tangles in subcortical areas were only rarely immunoreactive for 3R

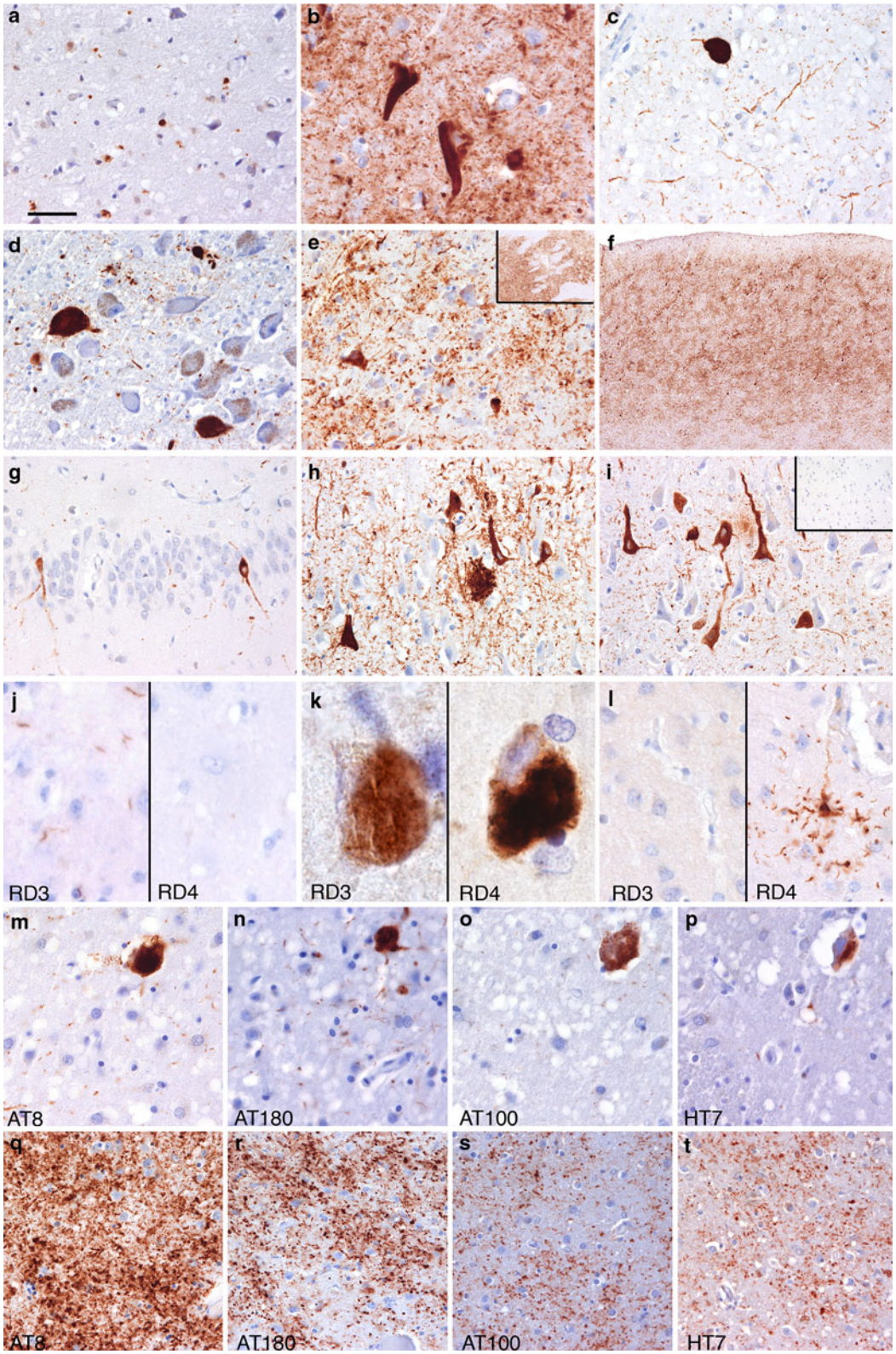

tau, but many were prominently 4R immunoreactive (Fig. 6k). In neocortical areas and hippocampus, both 3R and 4R immunopositivities were noted in neurofibrillary tangles. Thread-like structures were mainly 4R immunopositive (Fig. 6l) and were associated with neurofilaments but not astrocytic processes (Fig. 7b, c). In such areas, PrP

◀ **Fig. 6** Immunoreactivity for phosphorylated tau. **a** Neuritic profiles in the neuropil in areas with spongiform change (AT8. thalamus). **b** Neurofibrillary tangles in the temporal cortex (AT8). **c** Globose neurofibrillary tangles and threads in the putamen (AT8) and in the locus coeruleus (**d**). Prominent thread pathology and neuronal cytoplasmic immunoreactivity in the caudate nucleus (**e**, *right upper inset* shows overview) and in the frontal cortex (**f**) in a representative case (AT8). Diffuse neuronal cytoplasmic immunoreactivity in the granular layer of the dentate gyrus (**g**), in the CA2/3 subregion (**h**), and in the CA1 subregion (**i**) with thin thread and dots in the neuropil, and a relative sparing of the entorhinal cortex (**i**, *right upper inset*, all AT8). Neuritic profiles are immunoreactive mainly for 3R tau (**j**, *left side*), globose tangles in subcortical areas are immunoreactive for both 3R (**k**, *left side*) and 4R tau (**k**, *right side* of image), while cases with prominent thread-like pathology show mainly 4R immunoreactivity (**l**, *right side* of image). Representative images of a case with subcortical tauopathy (**m–p**) and one with prominent threads (**q–t**) immunostained with AT8 (**m**, **q**), AT180 (**n**, **r**), AT100 (**o**, **s**), and HT7 (**p**, **t**) antibodies. *Bar graph* indicates in **a** indicates 60 μm for **a–e**, **g–i**, and **m–t,** 1,000 μm for **f** and **e** upper inset; and 20 μm for **j–l**

deposition was also noted (Fig. 7d). We immunolabeled all these structures with anti-AT180, AT100, and HT7 antibodies (Fig. 6m–t), although neuritic profiles were less seen with HT7. AT8 and AT180 produced the most extensive immunoreactivity.

Immunoblotting for tau Four cases were examined: three cases (MM at codon 129) with only mild to moderate neuritic tau pathology, and one further case (MV at codon 129) with tau pathology in the cortex. In one case with mild dot-like neuritic immunoreactivity detected by the AT8 antibody in immunohistochemistry, western blotting of sarkosyl-insoluble tau using anti-tau AT8 antibody did not reveal immunopositivity. However, anti-tau antibody T46 showed immunoreactivity at 60 and 64 kDa in the frontal cortex and hippocampus (Fig. 8a, b). This was confirmed by the lack of labeling with RD4 and immunopositivity with the RD3 antibody (Fig. 8c, d) supporting our immunohistochemical observations with anti-RD3 and RD4. Both antibodies detected further small molecular weight bands. In one case with neurofibrillary tangles and glial tau immunoreactivity (MV at codon 129), AT8 and T46 showed patterns similar to AD (Fig. 8e) in the medial temporal lobe (hippocampus) sample, while 3R tau was detected in several regions examined (Fig. 8f). Unfortunately, frozen material was not available in cases with the unusual immunohistochemical patterns, predominated by 4R immunopositivity, of tau described above.

α-Synuclein pathology

Three types of α-synuclein pathology were observed: (1) typical Lewy bodies and Lewy neurites following Braak stages in six cases (15.4%) [4]; this consisted of three cases (aged 53, 66, and 66) with neocortical involvement (Braak V–VI) (Fig. 9a), two cases (aged 67 and 68) with limbic involvement (Braak IV), and one with brainstem involvement (aged 60) (Fig. 9b). (2) Prominent neuronal granular diffuse cytoplasmic immunoreactivity restricted to neurons of medullary raphe nuclei, dorsal vagus nucleus (Fig. 9c), locus coeruleus and substantia nigra; this was observed in 13 cases (including 4 with immunoreactivity only in the medulla oblongata) lacking Lewy bodies or Lewy neurites. Lower raphe nuclei and the dorsal vagus nucleus always showed the most prominent neuronal immunoreactivity, but scattered cortical neurons also showed this immunoreactivity. (3) Some areas showed small aggregates of α-synuclein in the neuropil reminiscent of that described in sporadic CJD [25]. However, this was not consistent and showed no region preference or relation to PrP deposition.

Deposition of Aβ

This included mainly diffuse deposits, some with multiple small cores, subpial and vascular deposition (Fig. 9d–f). Parenchymal deposits were mainly Aβ-42 and less Aβ-40 immunoreactive (Fig. 9h–i). Parenchymal Aβ was observed in 21 cases (53,8%) that involved frontal, temporal, and occipital regions in all, basal ganglia in five, and cerebellum in two. Cerebral amyloid angiopathy (Aβ-CAA) was noted in nine individuals (23.07%): this involved leptomeningeal and cortical vessels but not capillaries. Cored neuritic plaques were only occasionally seen and none of the cases fulfilled the criteria of AD according to CERAD [48]. The youngest patient with parenchymal Aβ deposition was 51 years old and the youngest individual with Aβ-CAA was 54.

Phosphorylated TDP-43, FUS, and ubiquitin immunohistochemistry

Immunostaining for FUS revealed variably strong staining of neuronal nuclei. We did not observe neuritic profiles or intracellular deposits in any case in the examined regions (Table 1). Similarly, in all cases there was a lack of phosphorylated TDP-43 pathology. Immunostaining for ubiquitin showed variable amount of granular immunoreactivity in the neuropil in severely affected areas along with neuritic profiles. Of note were the prominent perisomatic granules surrounding pyramidal neurons in the hippocampal CA1 subregion in 13 cases (33%).

Summary of proteinopathies

In addition to PrP, 36 cases (92.3%) showed some kind of concomitant protein deposition. Excluding the presence of neuritic tau pathology, co-pathology was seen in 32 cases (82%) (summarized in Table 3). Age at death and duration of illness did not differ between cases with and without

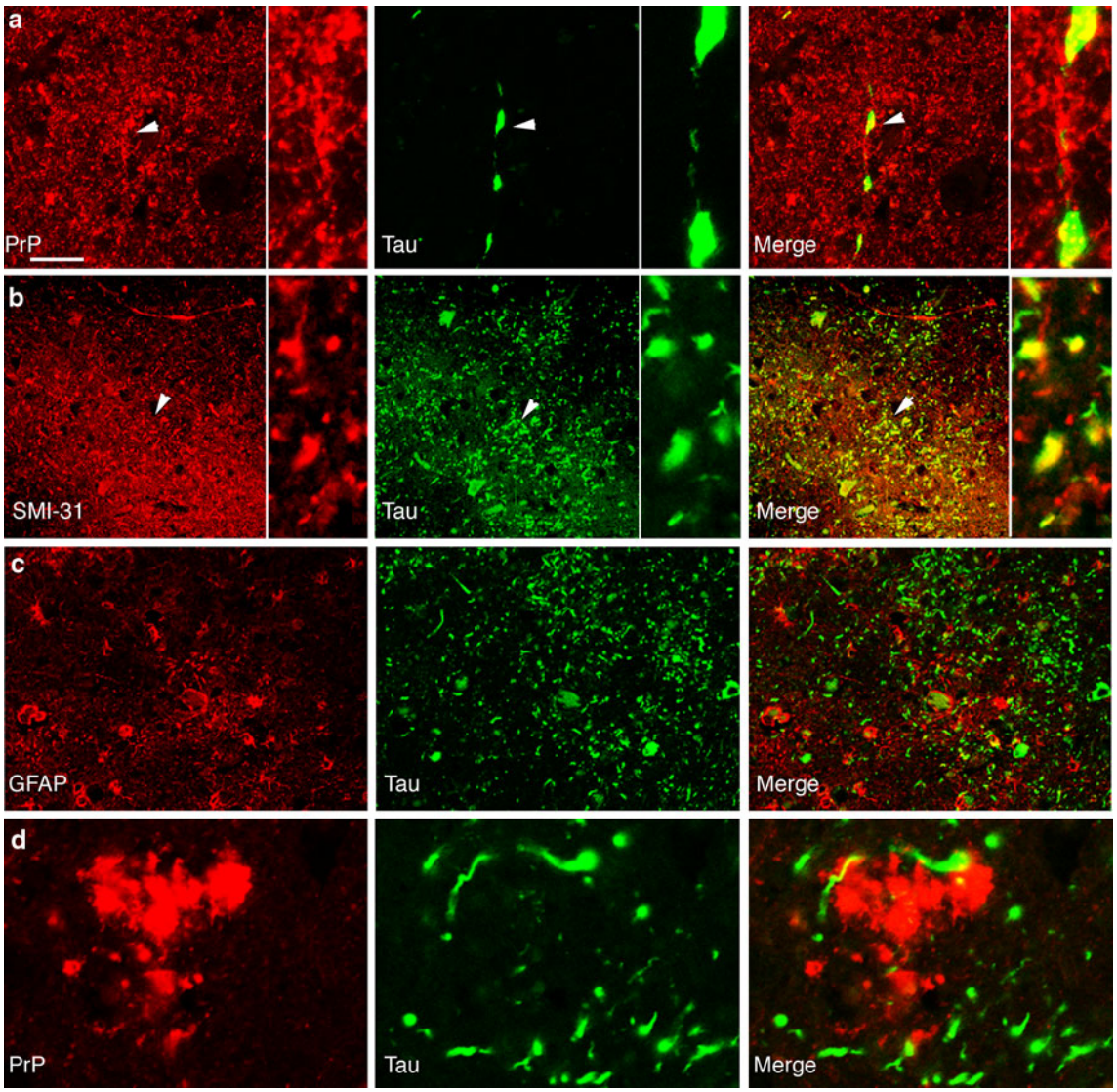

Fig. 7 Double immunolabeling in cases with tau pathology. Tau immunoreactive neurites occasionally co-localize with disease-associated PrP (**a**, AT8 *green*, PrP *red*, ×400; *arrowhead* indicates enlarged part in the right side of the images). Thread-like pathology associates with neurofilaments (**b**, AT8 *green*, SMI-31 *red*, ×400; *arrowhead* indicates enlarged part in the right side of the images) and not with astrocytic processes (**c**, AT8 *green*, GFAP *red*, ×400). In these areas PrP deposition is also noted (**d**, AT8 *green*, PrP *red*, ×1000). *Bar graph* in **a** indicates 60 μm in **a–c** and 15 μm in **d** and in enlarged insets of **a–c**

co-depositions, except for older age at death in cases with unclassifiable tauopathy (mean age ± standard error: 64.9 ± 1.7 versus 57.7 ± 1.7; $p = 0.016$). In cases with α-synucleinopathy, the patients already had neurological examination prior to rapidly progressive dementia, because of e.g. tremor of tongue, behavioral change, or typical Parkinsonism responding to L-Dopa therapy. In cases with tau pathology in the basal ganglia, dystonia, chorea or rigidity was noted, and in two cases supranuclear gaze palsy. In cases where memory impairment was indicated as a presenting symptom, neurofibrillary degeneration was noted. Otherwise the rapidly progressive clinical phase did not differ between cases with different protein depositions. There was no significant influence of the *PRNP* codon 129 polymorphism on concomitant proteinopathy. Protein co-depositions were noted in individuals from all countries included in our study.

Discussion

This study has the following implications: (1) genetic CJD with the E200K mutation is clinically characterized mostly by progressive dementia and ataxia and further symptoms, however, prominent supranuclear palsy, insomnia, and polyneuropathy may also be present. (2) E200K CJD

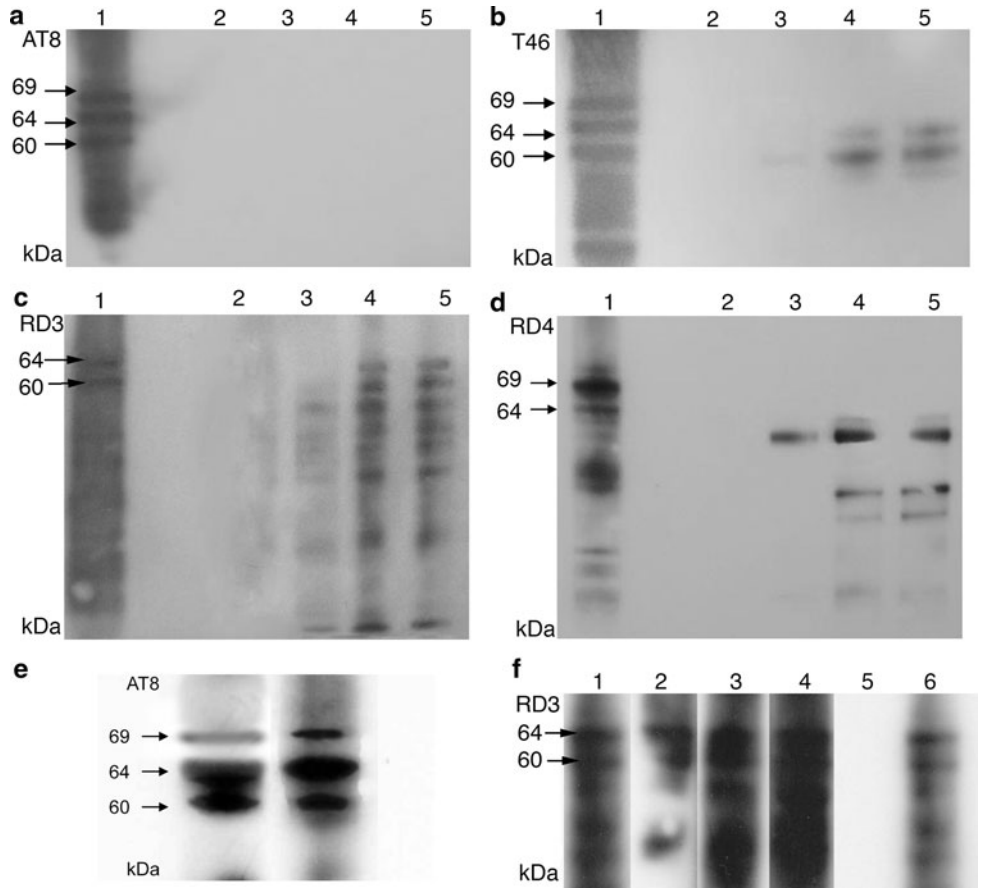

Fig. 8 Immunoblotting of sarkosyl-insoluble tau using different antibodies. **a** Immunostaining using AT8 anti-tau antibody did not reveal positive bands in a case with focal dot-like neuritic immunoreactivity observed in immunohistochemistry. **b** The same sample examined by T46 anti-tau antibody showed bands at 60 and 64 kDa molecular weight characteristic for 3R tau. Anti-RD3 (**c**) and anti-RD4 antibodies (**d**) showed different fragments of tau, and RD3 confirms the presence of 60 and 64 kDa bands. (*Lane 1* medial temporal cortex sample from a patient with Alzheimer's disease; *lane 2* medial temporal cortex sample from a non-diseased individual (examined by neuropathology); *lanes 3–5* Hungarian patient (MV at codon 129) with dot-like neuritic tau pathology detected in immunohistochemistry. *3* cerebellum, *4* frontal cortex, *5* temporal cortex. **e** Typical PHF-like pattern like in E200K CJD case etected by AT8 in medial temporal cortex (*Lane 1* medial temporal cortex including hippocampus from E200K CJD patient, *lane 2* Alzheimer's disease sample). **f** 3R tau were detected in several regions examined in case with neurofibrillary tangles restricted to the medial temporal lobe and neuritic tau pathology in the frontal and temporal cortices and striatum (*Lane 1* frontal cortex, *lane 2*: striatum, *lane 3*: medial temporal lobe including hippocampus, *lane 4*: temporal cortex, *lane 5* medial temporal cortex sample from a non-diseased individual, examined by neuropathology, *lane 6*: Alzheimer's disease sample)

presents with various PrP deposition patterns that frequently overlap between MM homozygotes and MV heterozygotes at *PRNP* codon 129. This is also reflected by a mixture of type 2 and type 1 PrP^{res} in these brains. (3) Lesion profiles do not differ significantly between MM and MV cases. (4) Some PrP deposition patterns are not seen in sporadic CJD or other genetic forms (e.g. stripe-like pattern in the cerebellum or distinct intraneuronal PrP aggregates involving prominently brainstem nuclei). Moreover, immunoblotting for PrP^{res} demonstrated distinct ratios of glycosylated to unglycosylated bands as compared to sporadic CJD. (5) Concomitant presence of α-synuclein, phospho-tau pathology or deposition of Aβ is more the rule than the exception. These protein deposits are present in areas where disease-associated PrP is also present.

Clinical features of E200K genetic CJD frequently overlap with that of sporadic CJD, including the presence of periodic sharp wave complexes. However, in our cohort myoclonus is less frequently documented. In spite of the less prominent pathology in the cerebellum, ataxia is often observed. Interestingly, the patterns of pathology observed in the cerebellum include either spongiform change and neuronal loss with diffuse/synaptic PrP immunoreactivity, or little lesioning associated with a stripe-like pattern of PrP immunoreactivity restricted to the molecular layer. This suggests that cerebellar ataxia may have a complex

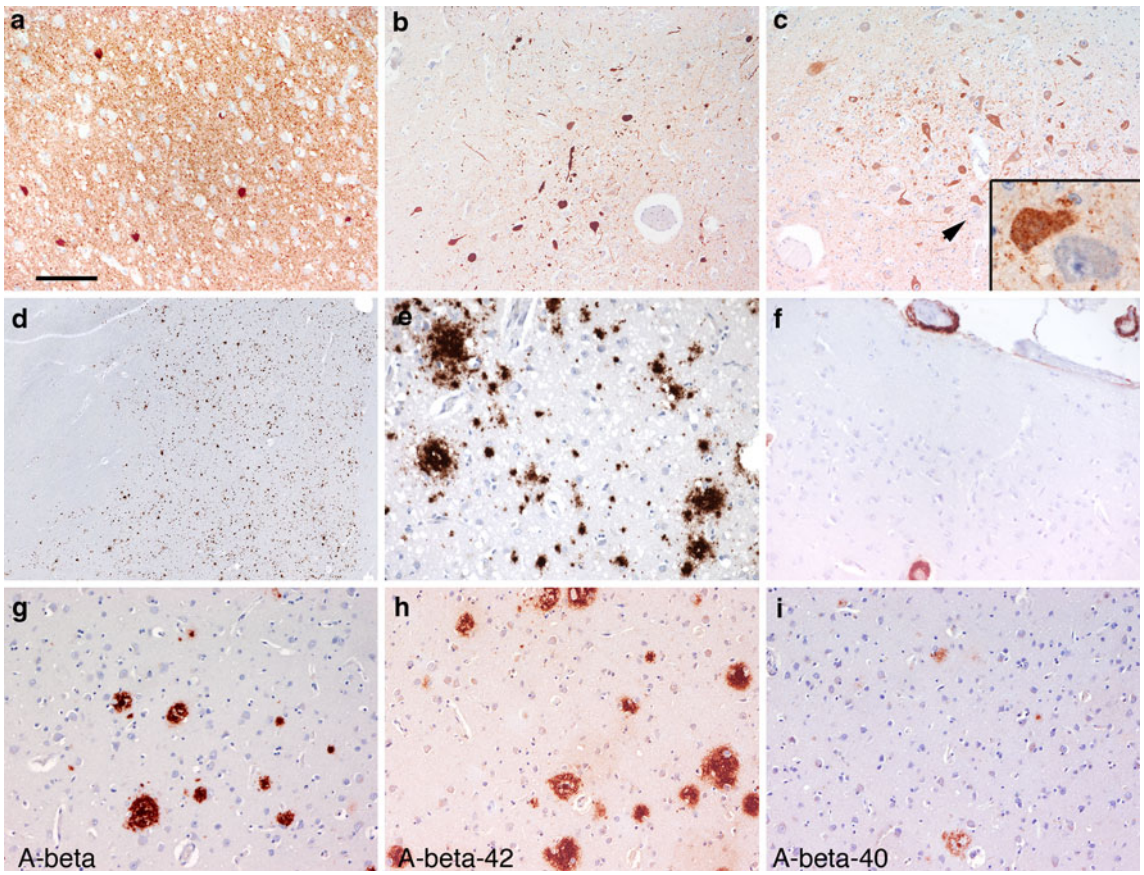

Fig. 9 Immunoreactivity for α-synuclein and amyloid-β (Aβ) in E200K genetic CJD. Typical α-synuclein immunopositive cortical Lewy bodies and Lewy neurites in the frontal cortex (**a**), and brainstem-type Lewy bodies in the medulla oblongata (**b**) in representative cases showing α-synuclein pathology compatible with Braak stageing. Prominent neuronal granular diffuse cytoplasmic immunoreactivity restricted to neurons of medullary raphe nuclei, dorsal vagus nucleus (**c**, cell indicated with arrowhead enlarged in *right lower inset*) but lacking Lewy bodies or Lewy neurites. Extensive Aβ deposition of the form of diffuse plaques and focal deposits in the striatum (**d**, **e**), and in the vessel walls in the frontal cortex (**f**) in representative cases. Parenchymal Aβ deposition (**g**) was mainly immunoreactive for anti-Aβ-42 (**h**) and less for anti-Aβ-40 (**i**) peptide. *Bar graph* in **a** indicates 200 μm for **a**, **f**, **g**, **h**, **i**, 150 μm for **e**, 400 μm for **b**, **c** (60 μm for inset), and 1,200 μm for **d**

background by either a more severe tissue damage of cerebellar cortical layers or, since the stripe-like pattern strongly resembles the compartmentalization of the cerebellar cortex and Purkinje cell branching [67], by alterations of synaptic contacts of Purkinje cells. In comparison with other cohorts [47, 63], chorea/dystonia was more frequently reported in our study than Parkinsonism. Similar to other reports, we confirm that supranuclear gaze palsy, insomnia, and polyneuropathy may be prominent in some cases [1, 2, 8, 50, 64]; this is not related to the codon 129 polymorphism. In our cohort, unusual clinical presentations like early memory impairment, supranuclear palsy, premorbid symptoms, or even characteristic Parkinson syndrome, years before the rapid progressive course, were described and frequently suggestive as substrate of concomitant protein deposition. However, due to the retrospective nature of our clinical data collection, it remains to be established how the presence of concomitant proteinopathies influence the clinical course. This merits further prospective studies, but it is clear that genetic CJD should be considered in less elderly patients (50–60 years) with a clinical suspicion of a pre-existing neurodegenerative disease (including "typical" Parkinson's disease) that switches into a rapidly progressive phase with dementia and ataxia.

Lesion profiles, defined by spongiform change and neuronal loss/gliosis, were not significantly different between cases with different constellation at codon 129. Of note was the variable involvement of neocortical areas, including frequent laminar accentuation, and the constant lesioning in the striatum and thalamic nuclei. The latter is reflected also in the signal alterations detected in MRI [15]. Sometimes the involvement of the thalamus may predominate, leading to further differential diagnostic issues [39]. In addition, neuronal loss was seen in the substantia nigra with or without α-synuclein inclusions. Nigrostriatal

Table 3 Summary of combinations of proteinopathies

Protein pathology	Unusual tauopathy	Tau-NFD-Braak	a-Synuclein-Braak	A-beta deposits	A-beta CAA	Number of cases	% of proteinopathy	% of all cases
Unusual tauopathy	0	+	−	−	−	4	33.3	10.2
Unusual tauopathy	0	−	+	−	−	5	41.6	12.8
Unusual tauopathy	0	−	−	+	−	6	50	15.3
Unusual tauopathy	0	−	−	−	+	4	33.3	10.2
Unusual tauopathy	0	+	+	−	−	3	25	7.7
Unusual tauopathy	0	+	+	+	−	2	16.6	5.1
Unusual tauopathy	0	+	+	−	+	0	0	0
Unusual tauopathy	0	+	−	−	+	0	0	0
Unusual tauopathy	0	+	+	+	+	1	8.3	2.5
α-Synuclein-Braak	+	−	0	−	−	5	83.3	12.8
α-Synuclein-Braak	−	+	0	−	−	3	50	7.7
α-Synuclein-Braak	−	−	0	+	−	4	66.6	10.2
α-Synuclein-Braak	−	−	0	−	+	2	33.3	5.1
α-Synuclein-Braak	−	+	0	+	−	2	33.3	5.1
α-Synuclein-Braak	−	+	0	−	+	1	16.6	2.5
α-Synuclein-Braak	−	+	0	+	+	1	16.6	2.5
α-Synuclein-Braak	+	+	0	+	+	1	16.6	2.5
Aβ deposits	−	+	−	0	−	9	40.9	23
Aβ deposits	−	−	−	0	+	8	36.3	20.5
Aβ deposits	−	+	−	0	+	1	4.5	2.5
Aβ deposits	−	+	+	0	+	1	4.5	2.5
Aβ deposits	+	+	−	0	+	0	0	0
Aβ deposits	+	+	+	0	+	1	4.5	2.5

The predominant proteinopathy is indicated in the left column and all further types of features that are additionally seen are indicated with a + sign

NFD neurofibrillary degeneration degeneration following Braak and Braak stageing, *CAA* cereberal amyloid angiopathy (Aβ)

damage was demonstrated in a recent study in sporadic CJD [66]. In contrast to the lesion profile, the morphology of PrP deposits showed more variation: more coarse immunodeposits (plaques, patchy/perivacuolar), but also more intraneuronal PrP aggregates were detected in cases with MV at codon 129 as compared to MMs. However, these deposits were frequently in MM cases in a more restricted distribution suggesting presence of different PrP types. Indeed, a mixture of type 1 and 2 PrP^{res} was observed in some cases. Regional variability between cerebral and cerebellar cortex of the PrP^{res} pattern was reported only in a single case [57]. We extend this finding by demonstrating variability in many regions in 2 out of 10 cases. Analysis of further 10 French cases with E200K mutation, not included in the present comprehensive neuropathological survey, revealed 3 cases with regional variability. According to these observations, a rough estimate of approximately 25% of cases with E200K mutation, slightly less than reported in sporadic CJD [54], shows this phenomenon. It was already reported that the western blot pattern of PrP^{res} in E200K genetic CJD differs from sporadic CJD [7, 27]. In spite of the presence of similar morphological immunodeposits, some PrP immunoreactive patterns were unusual (e.g. intraneuronal PrP immunopositivity) as a potential correlate of the distinct PrP^{res} patterns. Intraneuronal dot-like PrP immunoreactivity was reported in the E200K mutation [43] and V180I mutation also with abnormally glycosylated PrP^{res} [51], while intraneuronal PrP immunoreactivity (albeit morphologically not with dot-like accentuation) was documented in a patient with apparently sporadic CJD and novel glycotype pattern [69]. All together these observations suggest that the E200K mutation induces a relatively uniform anatomical pattern of tissue lesioning (spongiform change, neuronal loss/gliosis), while the deposition of disease-associated PrP is more influenced by the codon 129 constellation, including different types of, also mixed, PrP^{res} forms.

In addition, we detected a range of concomitant protein deposits. Tau pathology was represented either by the presence of small neuritic profiles, neurofibrillary degeneration following stages of Braak and Braak [3], or by

unusual forms that, based on the distinct anatomical distribution, lack of astrocytic plaques or tufted astrocytes, were not compatible with sporadic tauopathies. Interestingly, neurofibrillary tangles frequently occurred in brainstem nuclei (raphe, locus coeruleus) also in relatively young patients, analogously to that described as an early feature not only in AD but also in mild cognitive impairment [24, 62]. Neuritic profiles clustering around plaques are described in the acquired prion disease, variant CJD [19], while neurofibrillary tangles are consistent features of some *PRNP* mutations associated with prominent PrP amyloidosis [17]. Both features are not observed in E200K CJD. Interestingly, an unusual pattern of tauopathy was described in the R208H *PRNP* mutation associated with a CJD phenotype [59]. Double immunolabeling studies suggest that most of the tau pathology is neuronal in origin. Interestingly, AT8 and T46 antibodies showed different results in immunoblotting. Both antibodies were able to detect an AD-like pattern in samples where neurofibrillary degeneration was observed; however, in samples with mild neuritic profiles seen in immunohistochemistry, only T46 and RD3 antibody showed bands characteristic of 3R tau. Whereas postmortem delay and storage temperature may be a limitating factor for the detection of PHF and phosphorylated forms of tau [14, 60], in our study PHF and 3R tau were clearly detectable by western blot. However, immunoreactivity against specific phosphorylation sites may be reduced due to tau degradation by endogenous phosphatases. Thus, our observation on low molecular bands in a limited number of cases must be interpreted with caution and merits further evaluation on more cases whether a difference in epitopes or other factors might be the basis of this. In cases with unusual presentations of tau pathology, 4R isoform was prominently detected in immunohistochemistry, whereas in these cases no material was available for immunoblotting studies. However, it may be concluded that a spectrum of tau pathology from 3R through mixed and to 4R dominant forms is associated with the E200K mutation. In addition, Aβ deposition (parenchymal and vascular) frequently occurs in E200K genetic CJD [18]. In addition, we observed Lewy body pathology following Braak stages, and also prominent neuronal granular α-synuclein immunoreactivity in brainstem nuclei without Lewy bodies (together in around half of the patients). This indicates that pathological upregulation and eventual inclusion body formation of α-synuclein is an important feature in E200K genetic CJD, supporting a potential interactive role of PrP and α-synuclein. Interestingly, in spite of the lack of a role of codon 129 polymorphism on the susceptibility for the α-synucleinopathy Parkinson's disease [61], the clinical presentation may be influenced by this [23]. Finally, we did not detect any protein deposition using anti-FUS and phosphorylated TDP-43 antibodies. The latter is in line with a recent study in various forms of CJD [31]. The presence of various protein depositions, independent of the codon 129 polymorphism or PrP^{res} type, could support a concept of further genetic or epigenetic factors leading to various presentations in significantly different ages (ranging from early 30 to 70 years of age).

The processing of PrP overlaps with that of Aβ and α-synuclein, since it includes the endosomal–lysosomal system [38, 52]. Mutual interactions between tau, Aβ, and α-synuclein were documented [36]. Based on our observation of Lewy bodies or neurofibrillary tangles in our diagnostic work-up, we conducted a systematic evaluation of protein deposition and presented the first systematic demonstration of intensified and combined neurodegeneration in a genetic prion disease due to a single point mutation. The spectrum of protein depositions is distinct from that associated with PrP amyloid [17, 19] or sporadic CJD [11, 66]. The observation of Aβ deposition, neurofibrillary degeneration, and α-synucleinopathy in individuals from different countries, together with the detection of tauopathy forms, not compatible with sporadic tauopathies [6], suggests the interaction of mutated PrP with tau [68], Aβ [55], and also α-synuclein. Cellular PrP has been shown to regulate the production of Aβ and forms a complex [55] with full-length tau protein in vitro [68]. Moreover, there is a homologous region in PrP and α-synuclein, and interestingly, homologous peptides corresponding to this sequence can promote fibrillization of α-synuclein [13]. Finally, our observation of the frequent and unusual intraneuronal accumulation of PrP immunoreactivity indicates failed release from the cell and overwhelming of the protein processing system. In sum, our and previous studies suggest an altered metabolism and intracellular trafficking of mutated PrP that interferes with the processing of other proteins and leads to their pathological deposition. Thus, the E200K PrP mutation may become an important model to decipher the molecular interplay among neurodegeneration-associated proteins. Our observations also support a complex pathogenetic interplay in the background of E200K genetic CJD that may lead to differences in penetrance and clinical phenotype. Finally, our study suggests to clinicians the suspicion of genetic CJD when early onset neurological symptoms turn into a rapidly progressive phase.

Acknowledgments This study was performed in the frame of the EU FP6 Project Neuroscreen LSHB-CZ-2006-037719 contract No. 037719. We are grateful for the technical assistance of Irene Leisser, Gerda Ricken, Lenkeine Marianna, Katalin Ress, Rachel Plantier, Françoise Didier, and for the kind cooperation of collegues and families of patients supporting our Surveillance systems. RV is a senior clinical investigator of the Research Foundation-Flanders. LL

was supported by a grant of the Hungarian Scientific Research Fund (OTKA-NK78012).

Conflict of interest statement None.

References

1. Antoine JC, Laplanche JL, Mosnier JF, Beaudry P, Chatelain J, Michel D (1996) Demyelinating peripheral neuropathy with Creutzfeldt-Jakob disease and mutation at codon 200 of the prion protein gene. Neurology 46:1123–1127
2. Bertoni JM, Brown P, Goldfarb LG, Rubenstein R, Gajdusek DC (1992) Familial Creutzfeldt-Jakob disease (codon 200 mutation) with supranuclear palsy. JAMA 268:2413–2415
3. Braak H, Braak E (1991) Neuropathological stageing of Alzheimer-related changes. Acta Neuropathol 82:239–259
4. Braak H, Del Tredici K, Rub U, de Vos RA, Jansen Steur EN, Braak E (2003) Staging of brain pathology related to sporadic Parkinson's disease. Neurobiol Aging 24:197–211
5. Brown P, Galvez S, Goldfarb LG, Nieto A, Cartier L, Gibbs CJ Jr, Gajdusek DC (1992) Familial Creutzfeldt-Jakob disease in Chile is associated with the codon 200 mutation of the PRNP amyloid precursor gene on chromosome 20. J Neurol Sci 112:65–67
6. Cairns NJ, Bigio EH, Mackenzie IR, Neumann M, Lee VM, Hatanpaa KJ, White CL 3rd, Schneider JA, Grinberg LT, Halliday G, Duyckaerts C, Lowe JS, Holm IE, Tolnay M, Okamoto K, Yokoo H, Murayama S, Woulfe J, Munoz DG, Dickson DW, Ince PG, Trojanowski JQ, Mann DM (2007) Neuropathologic diagnostic and nosologic criteria for frontotemporal lobar degeneration: consensus of the Consortium for Frontotemporal Lobar Degeneration. Acta Neuropathol 114:5–22
7. Cardone F, Liu QG, Petraroli R, Ladogana A, D'Alessandro M, Arpino C, Di Bari M, Macchi G, Pocchiari M (1999) Prion protein glycotype analysis in familial and sporadic Creutzfeldt-Jakob disease patients. Brain Res Bull 49:429–433
8. Chapman J, Arlazoroff A, Goldfarb LG, Cervenakova L, Neufeld MY, Werber E, Herbert M, Brown P, Gajdusek DC, Korczyn AD (1996) Fatal insomnia in a case of familial Creutzfeldt-Jakob disease with the codon 200 (Lys) mutation. Neurology 46:758–761
9. Collinge J, Palmer MS, Campbell T, Sidle KC, Carroll D, Harding A (1993) Inherited prion disease (PrP lysine 200) in Britain: two case reports. BMJ 306:301–302
10. de Silva R, Lashley T, Gibb G, Hanger D, Hope A, Reid A, Bandopadhyay R, Utton M, Strand C, Jowett T, Khan N, Anderton B, Wood N, Holton J, Revesz T, Lees A (2003) Pathological inclusion bodies in tauopathies contain distinct complements of tau with three or four microtubule-binding repeat domains as demonstrated by new specific monoclonal antibodies. Neuropathol Appl Neurobiol 29:288–302
11. Debatin L, Streffer J, Geissen M, Matschke J, Aguzzi A, Glatzel M (2008) Association between deposition of beta-amyloid and pathological prion protein in sporadic Creutzfeldt-Jakob disease. Neurodegener Dis 5:347–354
12. DelleDonne A, Klos KJ, Fujishiro H, Ahmed Z, Parisi JE, Josephs KA, Frigerio R, Burnett M, Wszolek ZK, Uitti RJ, Ahlskog JE, Dickson DW (2008) Incidental Lewy body disease and preclinical Parkinson disease. Arch Neurol 65:1074–1080
13. Du HN, Li HT, Zhang F, Lin XJ, Shi JH, Shi YH, Ji LN, Hu J, Lin DH, Hu HY (2006) Acceleration of alpha-synuclein aggregation by homologous peptides. FEBS Lett 580:3657–3664
14. Ferrer I, Santpere G, Arzberger T, Bell J, Blanco R, Boluda S, Budka H, Carmona M, Giaccone G, Krebs B, Limido L, Parchi P, Puig B, Strammiello R, Strobel T, Kretzschmar H (2007) Brain protein preservation largely depends on the postmortem storage temperature: implications for study of proteins in human neurologic diseases and management of brain banks: a BrainNet Europe Study. J Neuropathol Exp Neurol 66:35–46
15. Fulbright RK, Hoffmann C, Lee H, Pozamantir A, Chapman J, Prohovnik I (2008) MR imaging of familial Creutzfeldt-Jakob disease: a blinded and controlled study. AJNR Am J Neuroradiol 29:1638–1643
16. Gelpi E, Heinzl H, Hoftberger R, Unterberger U, Strobel T, Voigtlander T, Drobna E, Jarius C, Lang S, Waldhor T, Bernheimer H, Budka H (2008) Creutzfeldt-Jakob disease in Austria: an autopsy-controlled study. Neuroepidemiology 30:215–221
17. Ghetti B, Piccardo P, Frangione B, Bugiani O, Giaccone G, Young K, Prelli F, Farlow MR, Dlouhy SR, Tagliavini F (1996) Prion protein amyloidosis. Brain Pathol 6:127–145
18. Ghoshal N, Cali I, Perrin RJ, Josephson SA, Sun N, Gambetti P, Morris JC (2009) Codistribution of amyloid beta plaques and spongiform degeneration in familial Creutzfeldt-Jakob disease with the E200K–129M haplotype. Arch Neurol 66:1240–1246
19. Giaccone G, Mangieri M, Capobianco R, Limido L, Hauw JJ, Haik S, Fociani P, Bugiani O, Tagliavini F (2008) Tauopathy in human and experimental variant Creutzfeldt-Jakob disease. Neurobiol Aging 29:1864–1873
20. Goedert M, Jakes R, Crowther RA, Cohen P, Vanmechelen E, Vandermeeren M, Cras P (1994) Epitope mapping of monoclonal antibodies to the paired helical filaments of Alzheimer's disease: identification of phosphorylation sites in tau protein. Biochem J 301(Pt 3):871–877
21. Goldfarb LG, Brown P, Mitrova E, Cervenakova L, Goldin L, Korczyn AD, Chapman J, Galvez S, Cartier L, Rubenstein R et al (1991) Creutzfeldt-Jacob disease associated with the PRNP codon 200Lys mutation: an analysis of 45 families. Eur J Epidemiol 7:477–486
22. Goldfarb LG, Mitrova E, Brown P, Toh BK, Gajdusek DC (1990) Mutation in codon 200 of scrapie amyloid protein gene in two clusters of Creutzfeldt-Jakob disease in Slovakia. Lancet 336:514–515
23. Gossrau G, Herting B, Mockel S, Kempe A, Koch R, Reichmann H, Lampe JB (2006) Analysis of the polymorphic prion protein gene codon 129 in idiopathic Parkinson's disease. J Neural Transm 113:331–337
24. Grudzien A, Shaw P, Weintraub S, Bigio E, Mash DC, Mesulam MM (2007) Locus coeruleus neurofibrillary degeneration in aging, mild cognitive impairment and early Alzheimer's disease. Neurobiol Aging 28:327–335
25. Haik S, Privat N, Adjou KT, Sazdovitch V, Dormont D, Duyckaerts C, Hauw JJ (2002) Alpha-synuclein-immunoreactive deposits in human and animal prion diseases. Acta Neuropathol 103:516–520
26. Hainfellner JA, Parchi P, Kitamoto T, Jarius C, Gambetti P, Budka H (1999) A novel phenotype in familial Creutzfeldt-Jakob disease: prion protein gene E200K mutation coupled with valine at codon 129 and type 2 protease-resistant prion protein. Ann Neurol 45:812–816
27. Hill AF, Joiner S, Beck JA, Campbell TA, Dickinson A, Poulter M, Wadsworth JD, Collinge J (2006) Distinct glycoform ratios of protease resistant prion protein associated with PRNP point mutations. Brain 129:676–685
28. Horiguchi T, Uryu K, Giasson BI, Ischiropoulos H, LightFoot R, Bellmann C, Richter-Landsberg C, Lee VM, Trojanowski JQ (2003) Nitration of tau protein is linked to neurodegeneration in tauopathies. Am J Pathol 163:1021–1031
29. Hsiao K, Meiner Z, Kahana E, Cass C, Kahana I, Avrahami D, Scarlato G, Abramsky O, Prusiner SB, Gabizon R (1991)

Mutation of the prion protein in Libyan Jews with Creutzfeldt-Jakob disease. N Engl J Med 324:1091–1097
30. Inoue I, Kitamoto T, Doh-ura K, Shii H, Goto I, Tateishi J (1994) Japanese family with Creutzfeldt-Jakob disease with codon 200 point mutation of the prion protein gene. Neurology 44:299–301
31. Isaacs AM, Powell C, Webb TE, Linehan JM, Collinge J, Brandner S (2008) Lack of TAR-DNA binding protein-43 (TDP-43) pathology in human prion diseases. Neuropathol Appl Neurobiol 34:446–456
32. Jarius C, Kovacs GG, Belay G, Hainfellner JA, Mitrova E, Budka H (2003) Distinctive cerebellar immunoreactivity for the prion protein in familial (E200K) Creutzfeldt-Jakob disease. Acta Neuropathol 105:449–454
33. Korczyn AD, Chapman J, Goldfarb LG, Brown P, Gajdusek DC (1991) A mutation in the prion protein gene in Creutzfeldt-Jakob disease in Jewish patients of Libyan, Greek, and Tunisian origin. Ann NY Acad Sci 640:171–176
34. Kosik KS, Orecchio LD, Binder L, Trojanowski JQ, Lee VM, Lee G (1988) Epitopes that span the tau molecule are shared with paired helical filaments. Neuron 1:817–825
35. Kovacs GG, Bakos A, Mitrova E, Minarovits J, Laszlo L, Majtenyi K (2007) Human prion diseases: the Hungarian experience. Ideggyogy Sz 60:447–452
36. Kovacs GG, Botond G, Budka H (2010) Protein coding of neurodegenerative dementias: the neuropathological basis of biomarker diagnostics. Acta Neuropathol 119:389–408
37. Kovacs GG, Budka H (2009) Molecular pathology of human prion diseases. Int J Mol Sci 10:976–999
38. Kovacs GG, Gelpi E, Strobel T, Ricken G, Nyengaard JR, Bernheimer H, Budka H (2007) Involvement of the endosomal-lysosomal system correlates with regional pathology in Creutzfeldt-Jakob disease. J Neuropathol Exp Neurol 66:628–636
39. Kovacs GG, Horvath S, Strobel T, Puskas M, Bakos A, Summers DM, Will RG, Budka H (2009) Genetic Creutzfeldt-Jakob disease mimicking variant Creutzfeldt-Jakob disease. J Neurol Neurosurg Psychiatry 80:1410–1411
40. Kovacs GG, Laszlo L, Bakos A, Minarovits J, Bishop MT, Strobel T, Vajna B, Mitrova E, Majtenyi K (2005) Increased incidence of genetic human prion disease in Hungary. Neurology 65:1666–1669
41. Kovacs GG, Puopolo M, Ladogana A, Pocchiari M, Budka H, van Duijn C, Collins SJ, Boyd A, Giulivi A, Coulthart M, Delasnerie-Laupretre N, Brandel JP, Zerr I, Kretzschmar HA, de Pedro-Cuesta J, Calero-Lara M, Glatzel M, Aguzzi A, Bishop M, Knight R, Belay G, Will R, Mitrova E (2005) Genetic prion disease: the EUROCJD experience. Hum Genet 118:166–174
42. Kovacs GG, Trabattoni G, Hainfellner JA, Ironside JW, Knight RS, Budka H (2002) Mutations of the prion protein gene phenotypic spectrum. J Neurol 249:1567–1582
43. Kovacs GG, Voigtlander T, Hainfellner JA, Budka H (2002) Distribution of intraneuronal immunoreactivity for the prion protein in human prion diseases. Acta Neuropathol 104:320–326
44. Lee HS, Sambuughin N, Cervenakova L, Chapman J, Pocchiari M, Litvak S, Qi HY, Budka H, del Ser T, Furukawa H, Brown P, Gajdusek DC, Long JC, Korczyn AD, Goldfarb LG (1999) Ancestral origins and worldwide distribution of the PRNP 200K mutation causing familial Creutzfeldt-Jakob disease. Am J Hum Genet 64:1063–1070
45. Mancuso M, Siciliano G, Capellari S, Orsucci D, Moretti P, Di Fede G, Suardi S, Strammiello R, Parchi P, Tagliavini F, Murri L (2009) Creutzfeldt-Jakob disease with E200K PRNP mutation: a case report and revision of the literature. Neurol Sci 30:417–420
46. Mead S, Webb TE, Campbell TA, Beck J, Linehan JM, Rutherfoord S, Joiner S, Wadsworth JD, Heckmann J, Wroe S, Doey L, King A, Collinge J (2007) Inherited prion disease with 5-OPRI: phenotype modification by repeat length and codon 129. Neurology 69:730–738
47. Meiner Z, Gabizon R, Prusiner SB (1997) Familial Creutzfeldt-Jakob disease. Codon 200 prion disease in Libyan Jews. Medicine (Baltimore) 76:227–237
48. Mirra SS, Heyman A, McKeel D, Sumi SM, Crain BJ, Brownlee LM, Vogel FS, Hughes JP, van Belle G, Berg L (1991) The consortium to establish a registry for Alzheimer's Disease (CERAD). Part II. Standardization of the neuropathologic assessment of Alzheimer's disease. Neurology 41:479–486
49. Mitrova E, Belay G (2002) Creutzfeldt-Jakob disease with E200K mutation in Slovakia: characterization and development. Acta Virol 46:31–39
50. Neufeld MY, Josiphov J, Korczyn AD (1992) Demyelinating peripheral neuropathy in Creutzfeldt-Jakob disease. Muscle Nerve 15:1234–1239
51. Nixon R, Camicioli R, Cervenakova L, Mastrianni J (2000) The PRNP-V180I mutation is associated with abnormally glycosylated PrPCJD and intracellular PrP accumulations. In: XIVth International Congress of Neuropathology Brain Pathol Birmingham, UK, p 670
52. Pan T, Kondo S, Le W, Jankovic J (2008) The role of autophagy-lysosome pathway in neurodegeneration associated with Parkinson's disease. Brain 131:1969–1978
53. Parchi P, Giese A, Capellari S, Brown P, Schulz-Schaeffer W, Windl O, Zerr I, Budka H, Kopp N, Piccardo P, Poser S, Rojiani A, Streichemberger N, Julien J, Vital C, Ghetti B, Gambetti P, Kretzschmar H (1999) Classification of sporadic Creutzfeldt-Jakob disease based on molecular and phenotypic analysis of 300 subjects. Ann Neurol 46:224–233
54. Parchi P, Strammiello R, Notari S, Giese A, Langeveld JP, Ladogana A, Zerr I, Roncaroli F, Cras P, Ghetti B, Pocchiari M, Kretzschmar H, Capellari S (2009) Incidence and spectrum of sporadic Creutzfeldt-Jakob disease variants with mixed phenotype and co-occurrence of PrPSc types: an updated classification. Acta Neuropathol 118:659–671
55. Parkin ET, Watt NT, Hussain I, Eckman EA, Eckman CB, Manson JC, Baybutt HN, Turner AJ, Hooper NM (2007) Cellular prion protein regulates beta-secretase cleavage of the Alzheimer's amyloid precursor protein. Proc Natl Acad Sci USA 104:11062–11067
56. Peoc'h K, Manivet P, Beaudry P, Attane F, Besson G, Hannequin D, Delasnerie-Laupretre N, Laplanche JL (2000) Identification of three novel mutations (E196K, V203I, E211Q) in the prion protein gene (PRNP) in inherited prion diseases with Creutzfeldt-Jakob disease phenotype. Hum Mutat 15:482
57. Puoti G, Rossi G, Giaccone G, Awan T, Lievens PM, Defanti CA, Tagliavini F, Bugiani O (2000) Polymorphism at codon 129 of PRNP affects the phenotypic expression of Creutzfeldt-Jakob disease linked to E200K mutation. Ann Neurol 48:269–270
58. Quadrio I, Ugnon-Cafe S, Dupin M, Esposito G, Streichenberger N, Krolak-Salmon P, Vital A, Pellissier JF, Perret-Liaudet A, Perron H (2009) Rapid diagnosis of human prion disease using streptomycin with tonsil and brain tissues. Lab Invest 89:406–413
59. Roeber S, Krebs B, Neumann M, Windl O, Zerr I, Grasbon-Frodl EM, Kretzschmar HA (2005) Creutzfeldt-Jakob disease in a patient with an R208H mutation of the prion protein gene (PRNP) and a 17-kDa prion protein fragment. Acta Neuropathol 109:443–448
60. Santpere G, Puig B, Ferrer I (2006) Low molecular weight species of tau in Alzheimer's disease are dependent on tau phosphorylation sites but not on delayed post-mortem delay in tissue processing. Neurosci Lett 399:106–110
61. Scholz SW, Xiromerisiou G, Fung HC, Eerola J, Hellstrom O, Papadimitriou A, Hadjigeorgiou GM, Tienari PJ, Fernandez HH, Mandel R, Okun MS, Gwinn-Hardy K, Singleton AB (2006) The

human prion gene M129V polymorphism is not associated with idiopathic Parkinson's disease in three distinct populations. Neurosci Lett 395:227–229
62. Simic G, Stanic G, Mladinov M, Jovanov-Milosevic N, Kostovic I, Hof PR (2009) Does Alzheimer's disease begin in the brainstem? Neuropathol Appl Neurobiol 35:532–554
63. Simon ES, Kahana E, Chapman J, Treves TA, Gabizon R, Rosenmann H, Zilber N, Korczyn AD (2000) Creutzfeldt-Jakob disease profile in patients homozygous for the PRNP E200K mutation. Ann Neurol 47:257–260
64. Taratuto AL, Piccardo P, Reich EG, Chen SG, Sevlever G, Schultz M, Luzzi AA, Rugiero M, Abecasis G, Endelman M, Garcia AM, Capellari S, Xie Z, Lugaresi E, Gambetti P, Dlouhy SR, Ghetti B (2002) Insomnia associated with thalamic involvement in E200K Creutzfeldt-Jakob disease. Neurology 58:362–367
65. Togo T, Sahara N, Yen SH, Cookson N, Ishizawa T, Hutton M, de Silva R, Lees A, Dickson DW (2002) Argyrophilic grain disease is a sporadic 4-repeat tauopathy. J Neuropathol Exp Neurol 61:547–556
66. Vital A, Fernagut PO, Canron MH, Joux J, Bezard E, Martin-Negrier ML, Vital C, Tison F (2009) The nigrostriatal pathway in Creutzfeldt-Jakob disease. J Neuropathol Exp Neurol 68:809–815
67. Voogd J, Glickstein M (1998) The anatomy of the cerebellum. Trends Neurosci 21:370–375
68. Wang XF, Dong CF, Zhang J, Wan YZ, Li F, Huang YX, Han L, Shan B, Gao C, Han J, Dong XP (2008) Human tau protein forms complex with PrP and some GSS- and fCJD-related PrP mutants possess stronger binding activities with tau in vitro. Mol Cell Biochem 310:49–55
69. Zanusso G, Polo A, Farinazzo A, Nonno R, Cardone F, Di Bari M, Ferrari S, Principe S, Gelati M, Fasoli E, Fiorini M, Prelli F, Frangione B, Tridente G, Bentivoglio M, Giorgi A, Schinina ME, Maras B, Agrimi U, Rizzuto N, Pocchiari M, Monaco S (2007) Novel prion protein conformation and glycotype in Creutzfeldt-Jakob disease. Arch Neurol 64:595–599